Structural Engineering and Mechanics, Vol. 35, No. 2 (2010) 241-256 241
DOI: http://dx.doi.org/10.12989/sem.2010.35.2.241

Numerical analyses of the force transfer in concrete-filled steel tube columns

Uwe Starossek, Nabil Falah* and Thomas Löhning

Structural Analysis and Steel Structures Institute, Hamburg University of Technology (TUHH), Denickestrasse 17, D-21073 Hamburg, Germany

(Received September 3, 2008, Accepted January 18, 2010)

Abstract. The interaction between steel tube and concrete core is the key issue for understanding the behavior of concrete-filled steel tube columns (CFTs). This study investigates the force transfer by natural bond or by mechanical shear connectors and the interaction between the steel tube and the concrete core under three types of loading. Two and three-dimensional nonlinear finite element models are developed to study the force transfer between steel tube and concrete core. The nonlinear finite element program ABAQUS is used. Material and geometric nonlinearities of concrete and steel are considered in the analysis. The damage plasticity model provided by ABAQUS is used to simulate the concrete material behavior. Comparisons between the finite element analyses and own experimental results are made to verify the finite element models. A good agreement is observed between the numerical and experimental results. Parametric studies using the numerical models are performed to investigate the effects of diameter-to-thickness ratio, uniaxial compressive strength of concrete, length of shear connectors, and the tensile strength of shear connectors.

Keywords: composite columns; concrete-filled steel tube; bond stress; load transfer; mechanical shear connectors; confinement; test; finite element analysis; parametric study.

1. Introduction

The concrete-filled steel tube (CFT) system has many advantages compared with the ordinary steel or the reinforced concrete systems. The enhancement in structural properties is due to the interaction between steel tube and concrete core. The confinement created by the steel casing enhances the material properties of concrete due to the triaxial state of stress. Conversely, the inward buckling of the steel tube is prevented by the concrete, thus increasing the stability and strength of the column as a system. In addition to these advantages, the steel tubes surrounding the concrete columns eliminate the need for formwork, which reduces construction time and costs.

The stress transfer between the concrete core and steel tube is necessary to develop composite action and achieve the full stiffness and resistance of CFT columns. The force can be transferred between the steel tube and concrete core either by natural bond between steel and concrete or by mechanical transfer devices. Many studies on the bond strength by means of push-out tests have been reported in the literature; among many examples are those of Virdi and Dolwling (1980), Roik

*Corresponding author, Ph.D., E-mail: falah@tuhh.de

et al. (1984), Shaker-Khalil (1991, 1993a, b) and Roeder *et al.* (1999). Although a large number of push-out tests available in the literature, they provide limited information on the real bond behavior in CFT columns (Johansson 2003). The main reason is that push-out tests do not represent the loading condition in an actual CFT column.

Concerning the design of CFTs, current design codes and standards assume that there is complete interaction (perfect bond) between steel and concrete. The ultimate value for bond stress is given as 0.4 MPa in Eurocode 4; the assumed transfer length of shear force should not exceed twice the smaller one of the two overall cross-sectional dimensions. If the acting bond stress exceeds the admissible mechanical shear connectors have to be inserted. However, there are no rational rules for determining how and where shear connectors are installed at the interface between concrete core and steel tube. There is still a shortage of information on the performance of shear connectors in such composite members. In continuous CFT columns with small cross-sectional dimensions, it is difficult to arrange mechanical shear connectors inside the tube in the regions where the highest transfer stresses occur.

The finite element technique has become a powerful tool for analyzing structures. Although experiments play a significant role in research on CFT columns, they are expensive and time consuming. Finite element analysis provides supplementary information to the experiments. Therefore, a detailed analysis of CFTs using finite element analysis is a useful approach as long as the numerical model is calibrated with experimental results.

The main objective of the present study is to investigate the force transfer between concrete core and steel tube by natural bond or by mechanical shear connectors and the interaction between the steel tube and the concrete core in CFTs by using the finite element method. The general-purpose finite element program ABAQUS is used in the analysis.

2. Experimental program

The test series consisted of 71 short columns tested to failure under centric axial loading (Falah 2008). The load is applied at the top of column to the steel section "S type of loading", to the concrete section "SP type of loading", to the entire section "A type of loading", whereas the steel

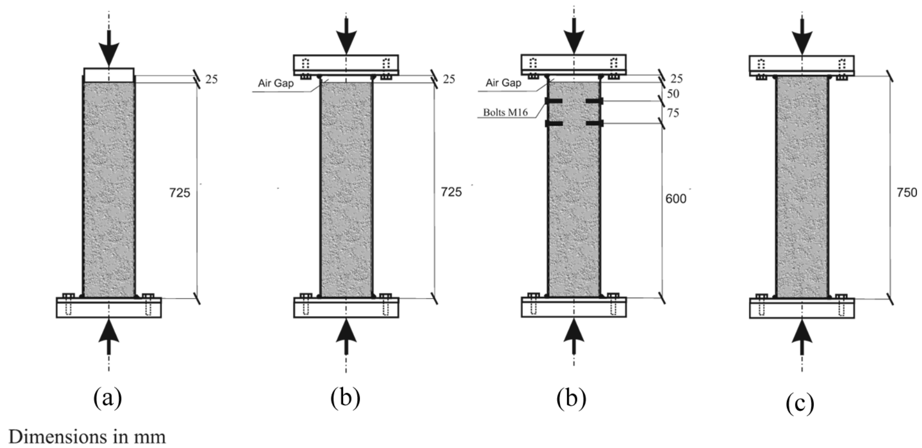

Fig. 1 (a) SP type of loading, (b) S type of loading, (c) A type of loading tube and concrete core are supported simultaneously at the bottom of the test specimen. For all types of loading the loading process is performed under displacement-controlled type of loading. Fig. 1 shows schematically the loading method. The axial deformations of specimens are measured by four linear variable differential transducers (LVDTs) with an accuracy of 0.001 mm. They are installed on each side of the top end plate. The longitudinal and circumferential strains of steel tube are measured by electrical strain gauges. Eighteen strain gauges are installed in the longitudinal direction in two columns (9 on each column), four strain gauges in the transverse direction in two rows (two on each row). The longitudinal strains of concrete core are measured by three embedded strain gauges. The test setup and instrumentations of test specimen are shown in Fig. 2. The

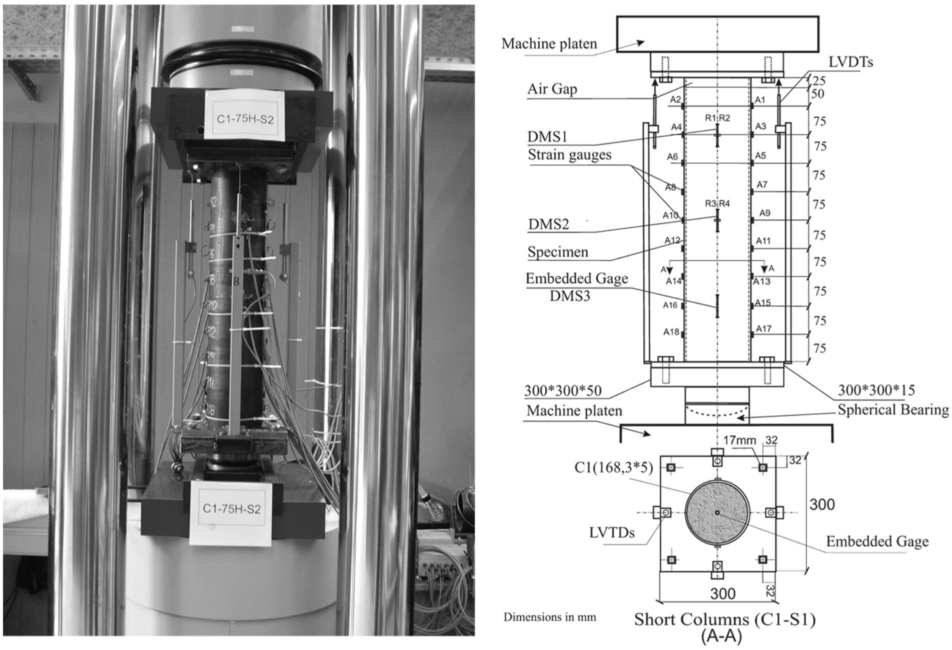

Fig. 2 Test setup and instrumentation of test specimen

Table 1 Properties of specimens

No	Designation	Dimension (mm)	Length (mm)	Steel f_y (MPa)	Concrete f_c (MPa)	Bond stress	Shear connector	Type of loading
1	C1-S	168.3×5	750	487	35	Yes	-	S
2	C1-4B-Sc	168.3×5	750	511	46	Yes	4 bolts	S
3	C1-UD-2B-Sc	168.3×5	750	487	35	No	2 bolts	S
4	C1-UD-4B-Sc	168.3×5	750	487	35	No	4 bolts	S
5	C1-A	168.3×5	750	487	35	Yes	-	A
6	C1-A	168.3×5	750	511	46	Yes	-	A
7	C1-A	168.3×5	750	511	74	Yes	-	A
8	C1-SP	168.3×5	750	487	44	Yes	-	SP
9	C2-A	244.5×7.1	750	411	32	Yes	-	A
10	C3-A	114.3×5	750	475	32	Yes	-	A
11	S1-A	150×150×6.3	750	411	32	Yes	-	A

Table 2 Properties of concrete

Density (kg/m³)		Compressive strength f_{cu} (MPa)		Modulus of elasticity E_c (MPa)
Cube 150×150×150	Cylinder Ø150/300	Cube 150×150×150	Cylinder Ø150/300	
2370	2360	55.1	46	31200
2300	2340	38.2	32	28200
2300	2320	48.5	35	28400
2330	2360	57.9	44	32600
2400	2410	87.6	74	40800

Table 3 Properties of steel tube obtained from coupon tests

Steel tube	Yield stress f_y (MPa)	Ultimate stress f_u (MPa)	Modulus of elasticity E_s (MPa)	Strain at yield E_y (%)	Elongation (%)
168.3×5	487	594	210168	0.242	24
168.3×5	511	626	189223	0.348	21
244.5×7.1	411	497	195998	0.223	32
114.3×5	475	592	187192	0.386	24
150×150×6.3	411	516	205094	0.225	32

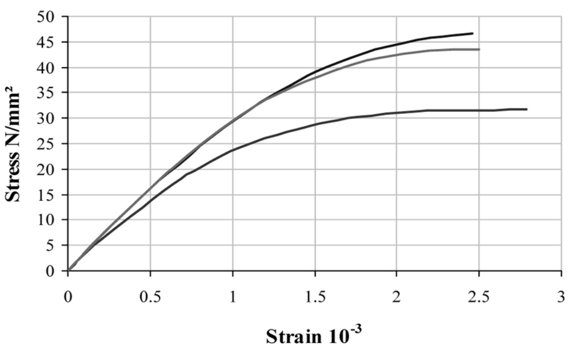

Fig. 3 Stress-strain curves for concrete

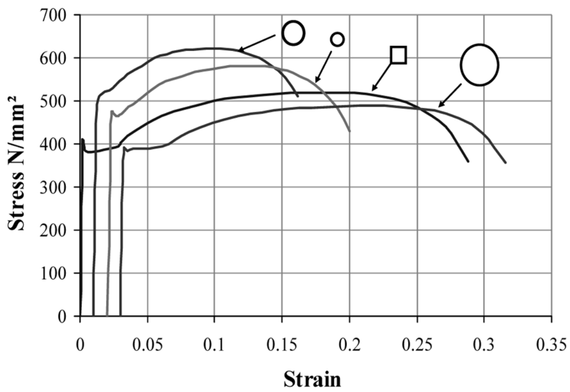

Fig. 4 Stress-strain curves obtained from coupon tensile test

material properties of concrete at the age of 28 days are given in Table 2, which were obtained from testing of six cylinders (Ø150/300) and three cubes (150 × 150 × 150). The stress-strain relationship for concrete is shown in Fig. 3. Three tension coupons are cut, and machined from the side of steel tube, and are tested in uniaxial tension in order to determine the mechanical properties of steel tube. The average values of tension test results are given in Table 3, and typical stress-strain curves for these tests are illustrated in Fig. 4. The details and properties of the specimens, modeled in the current study, are shown in Table 1.

3. Numerical modeling

In the field of structural engineering, results of finite element analysis may provide detailed information on the stress and the strain distributions in structures. Such information is not easily available from experiments, and, therefore, numerical investigation may be used to provide supplementary data for improved understanding. Furthermore, parametric studies on the finite element models may be performed to improve the efficiency of structural design. In recent years, advancements in FE formulation have produced robust algorithms to deal with complex geometry, large deformation, plasticity, and contact interaction. In this paper, two and three-dimensional materially and geometrically nonlinear finite element models are developed using the commercial finite element program ABAQUS/Standard 6.7. Two-dimensional axisymmetric models are used to model the concrete-filled steel tube column with circular cross section under A type of loading, and S type of loading without shear connectors. Three-dimensional models are used to model a quarter of concrete-filled steel tube columns with square cross section under A type of loading, and circular cross section under S type of loading with shear connectors.

3.1 Finite element mesh

Two-dimensional axisymmetric models are used to model the concrete-filled steel tube column with circular cross section. The concrete core, steel tube, and end plates are modeled using CAX4I axisymmetric solid element. The axisymmetric element is defined by four nodes having two degrees of freedom at each node; translations in the nodal z and r directions (Fig. 5). Because of the symmetry of the square columns and the circular columns, which are provided with shear connectors, only a quarter of the column is modeled using three-dimensional solid elements. In the modeling of the concrete core, steel tube, bolts, and end plates a three-dimensional eight-node element C3D8 with three degree of freedom at each node is used as shown in Fig. 5. CAX4I and C3D8 elements are available in the ABAQUS elements library. The finite element meshes for both circular and square sections are shown in Fig. 6.

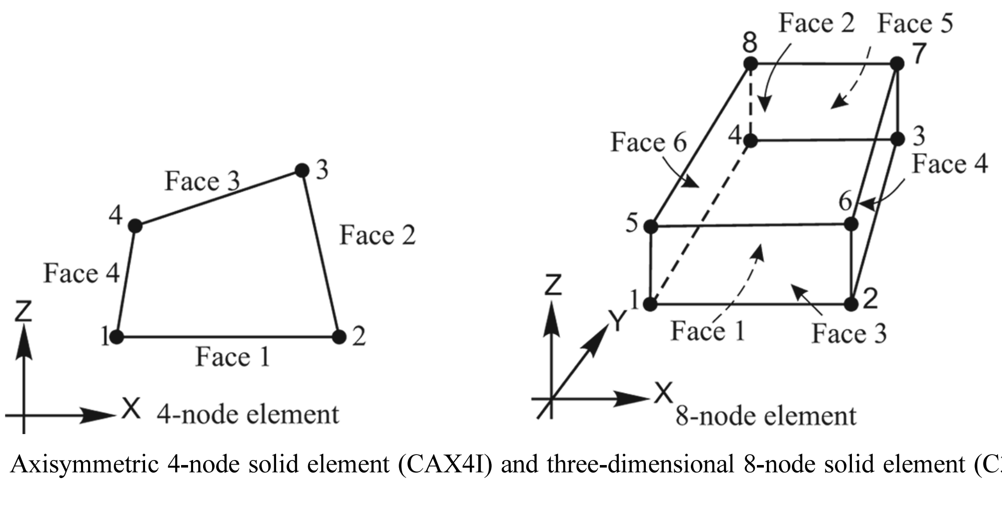

Fig. 5 Axisymmetric 4-node solid element (CAX4I) and three-dimensional 8-node solid element (C3D8)

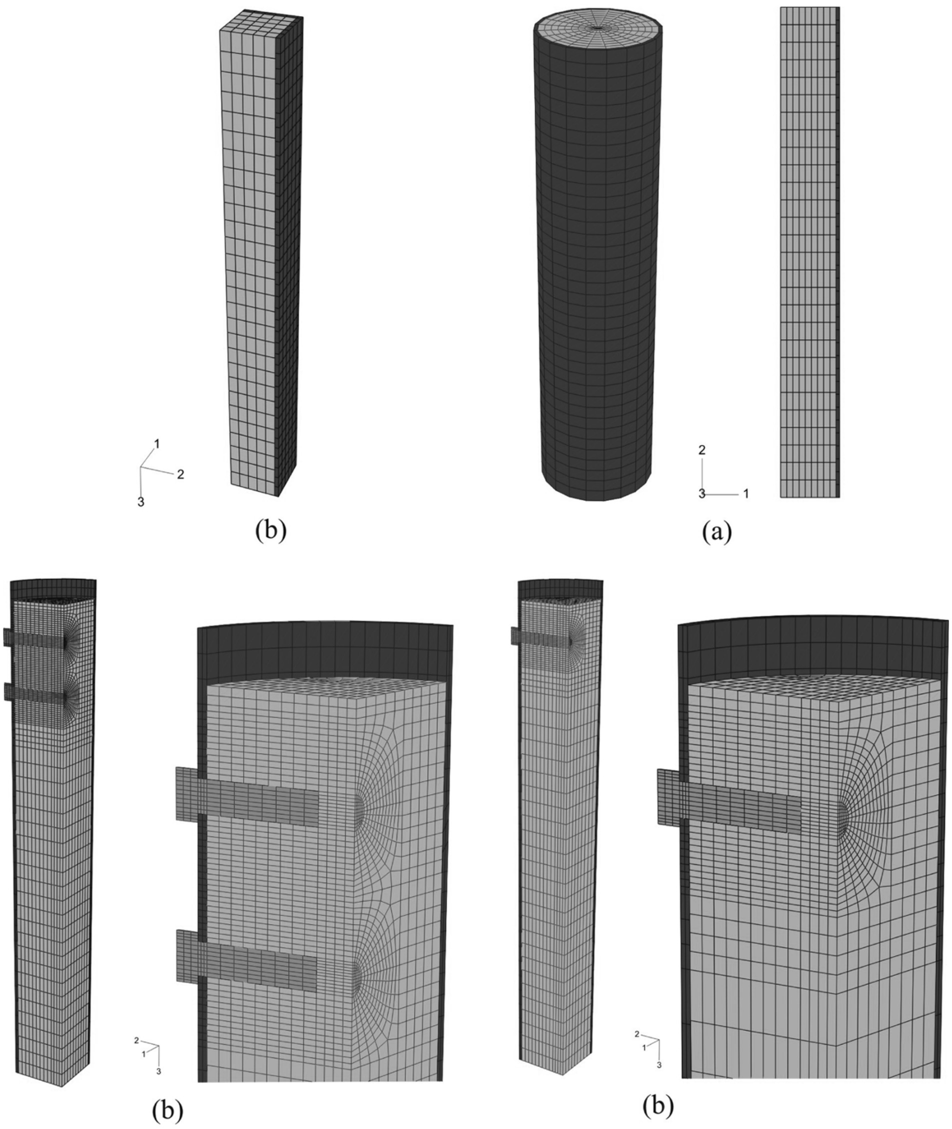

Fig. 6 Finite element mesh (a) two-dimensional model, (b) three-dimensional models

3.2 Material models

3.2.1 Concrete

The damaged plasticity model in ABAQUS is used to simulate the concrete behavior in the concrete-filled steel tube columns. The model is a three-dimensional continuum plasticity-based damaged model for concrete (Lubliner *et al.* 1989, Lee and Fenves 1998) that is capable of predicting both compressive and tensile behavior of concrete under confining pressure. The yield function is formulated in terms of effective hydrostatic pressure and the Mises equivalent effective stress and depends on two hardening variables. The two hardening variables are the integrated plastic strain rates separated into tension and compression. The user governs the shape of the yield surface by the two parameters K_c and $\sigma_{b0}/\sigma_{c0.}$ The first describes the shape of the deviatoric plane, the latter defines the ratio of initial equibiaxial to uniaxial compressive yield stress. The model uses a non-associated plastic flow rule to describe the plastic strain increments. The flow potential follows the Drucker-Prager hyperbolic function. The dilation angle for concrete defines the plastic strain direction with respect to the deviatoric stress axis in the rendulic plane. In this study, a value of 15° is used for the dilation angle of concrete. Damage characterizes the stiffness degradation for the unloading response. Due to the static loading, the damage effect can be neglected here. The numerically complex computation of the material model can be stabilized by viscoplastic regularization, which allows stresses outside the yield surface. The user can overcome convergence difficulties by defining a small viscosity parameter (e.g., μ = 0.00025). The uniaxial compressive stress-strain curve of concrete obtained from the standard cylinder tests is used (Fig. 3). In these tests the stress-strain relation is only registered to the maximum stress. The remaining part of the stress-strain relation is taken as perfect plastic line. The tension stiffening model is used to define cracking and postcracking properties for the concrete. The model assumes that the direct stress across a crack gradually reduces to zero as the crack opens. Tension stiffening is defined in the present study using stress-strain data. The stress-strain relationship as shown in Fig. 7 assumes that the tensile stress increases linearly with an increase in tensile strain up to concrete cracking. After concrete cracking, the tensile stress decreases linearly to zero as the concrete softens. For the tension stiffening effect, the reduction of concrete tensile strength to zero is assumed to occur at 10 times the strain at failure. The concrete tensile strength f_{ct} used in the analysis is determined as proposed by DIN-1045-1 (2001) and Poisson's ratio was υ = 0.2. The modulus of elasticity is taken as shown in Table 3.

3.2.2 Steel

An elastic-plastic model with the von Mises yield criterion is used to describe the constitutive behavior of steel tube. The complete stress-strain relation obtained from uniaxial tension-coupon tests has been used in steel material model (Fig. 4). The Poisson's ratio is taken as υ = 0.3. The material behavior of the bolt is described by bilinear stress-strain curve shown in Fig. 8 for

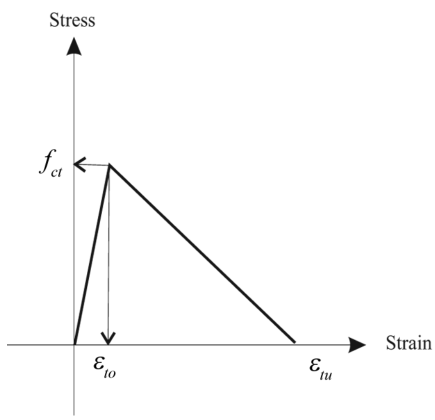

Fig. 7 Stress-strain curve for concrete in tension

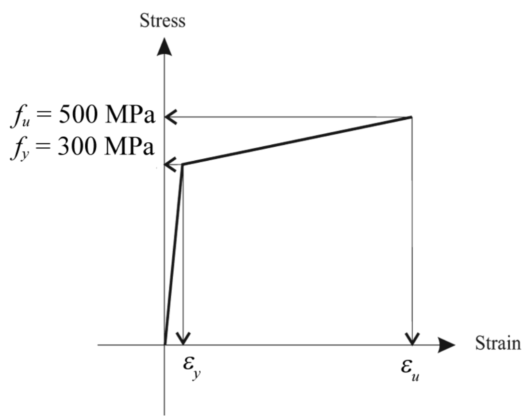

Fig. 8 Idealized stress-strain relationship for bolt material

compression and tension and an ultimate strain of 0.2 is used. Material properties of steel bolt, such as the Young's modulus and Poisson's ratio are taken as $E_s = 210000$ MPa and $\upsilon = 0.3$, respectively.

3.3 Interaction between steel and concrete

For the modeling of the CFT the interaction of the three members tube, concrete core, and bolt have to be considered. ABAQUS provides two methods for the modeling of contact, either surface contact or contact elements. The element-based deformable surface is used to define all required surfaces. A surface-based interaction with a contact pressure-overclosure model has been used. When surfaces are in contact they transfer shear forces as well as normal forces across their interface. A surface-based interaction with a contact pressure-overclosure model in the normal direction, and a nonlinear spring elements in the tangential directions between surfaces of steel tube and concrete core have been used for S type of loading. In this way the surfaces are able to separate and slide relatively to each other and to transmit contact pressure and shear stresses between concrete core and steel tube. The type of spring element is spring2 which is available in the ABAQUS/standard. The applied spring2-tpye is defined by two nodes and acts only in a fixed direction. The nonlinear spring behavior is specified by pairs of force-relative displacement values. The stiffness of springs has been determined by comparing numerical results with experimental ones. The contact pair option is used to specify which pairs of surfaces can interact with each other during the analysis. The contact condition between two surfaces is defined by using a strict master-slave algorithm. Surface-to-surface discretization prevents master nodes from undetected, distinctly penetration into the slave surface. The surface with the more refined surface is chosen as slave surface.

For the concrete-bolt and concrete-tube connections in the specimens with shear connectors, friction is considered with different friction coefficient. For the screw thread of the bolt a higher friction coefficient can be assumed (e.g., 0.4, 0.6). The screw connection between bolt and tube is presumed as to be tied together, so there is no relative displacement.

3.4 Boundary condition and load application

The nodes at the top and bottom surface of the concrete-filled steel tube columns are restrained in all degrees of freedom. For square cross sections, and circular cross sections with bolts, all concrete nodes and steel tube nodes, and bolt nodes in the symmetric planes are restrained perpendicular to these planes. In this study it was of interest to follow the ultimate behavior of the columns so the load is applied as static uniform load using the displacement control on the top surface. The displacement in the vertical direction is applied in incremental steps. The load was applied to the concrete section "SP type of loading", to the steel section "S type of loading", or to the entire section "A type of loading" at the top of column.

3.5 Verification of finite element models

Before a parametric study can be carried out, it is necessary to prove that the established finite element models are capable of simulating the structural behavior of concrete-filled steel tube columns, including the load transfer between concrete core and steel tube. A comparison of the numerical analyses results and the experimental results is carried out to verify the finite element

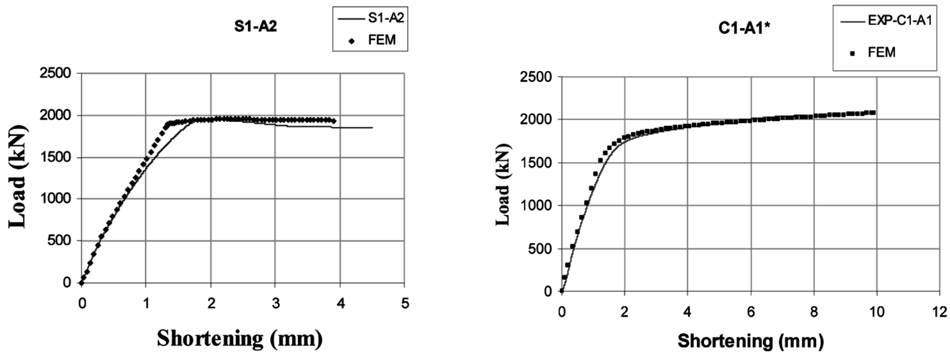

Fig. 9 Comparison between experimental and FEM results under A type of loading

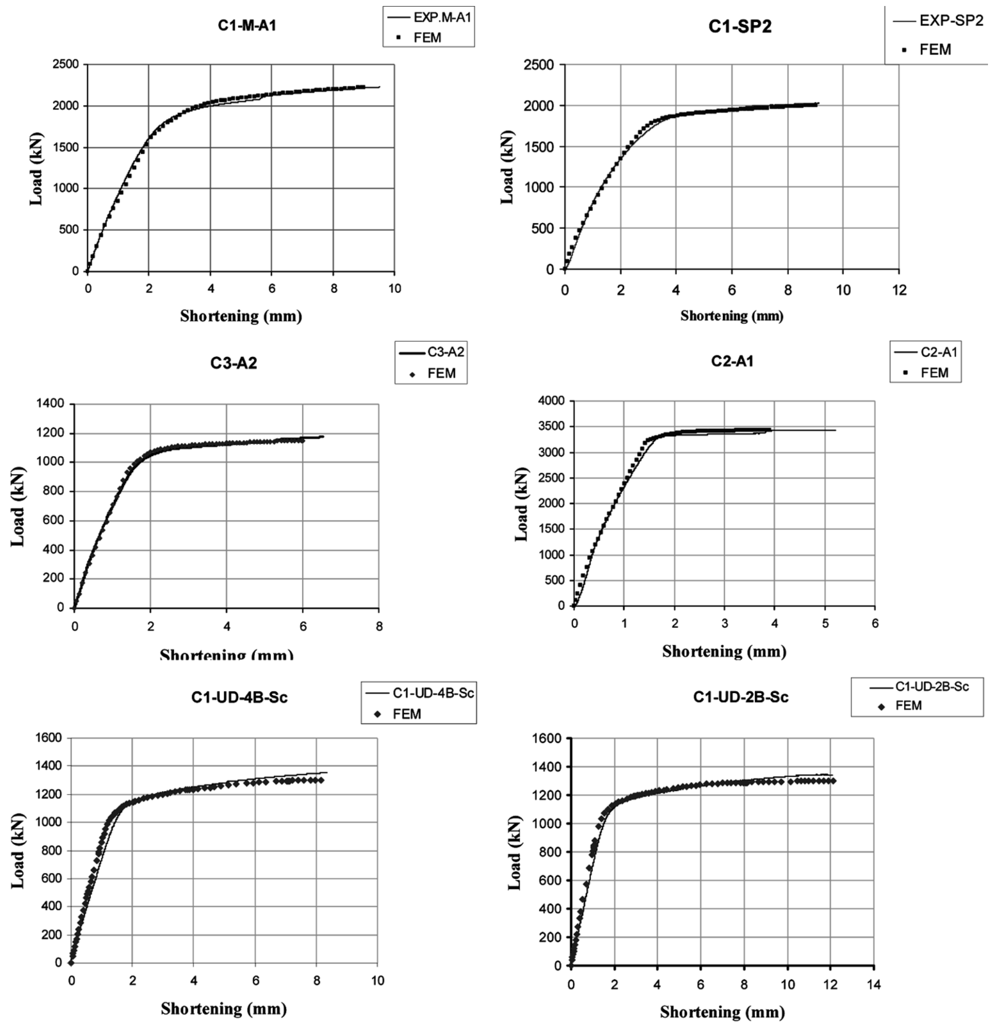

Fig. 10 Comparison between experimental and FEM results under A and SP type of loading

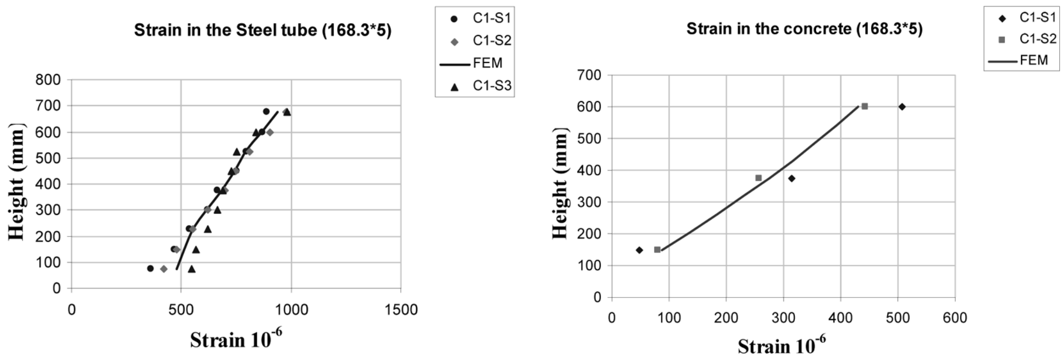

Fig. 11 Comparison between experimental and FEM results under S type of loading

models. In Figs. 9 and 10 the comparison between load-axial shortening curves obtained by numerical and experimental studies is presented. The average strain distribution in steel tube and concrete core along longitudinal axis at the maximum bond stress under S type of loading obtained by FE-analyses are compared with the experimental results (Fig. 11). It can be observed that, generally the results of finite element analysis are in good agreement with experimental data. After verification of the present finite element models, a comprehensive detailed analysis is performed on CFT columns.

4. Parameter study

Several basic parameters have significant impact on the behavior of confined concrete core or generally on the mechanical behavior of concrete-filled steel tube columns such as diameter to thickness ratio (*D/t*), uniaxial compressive strength of concrete, the level of applied lateral confinement pressure, and cross-sectional shape. Experimental investigation on the effect of all these parameter is practically difficult, since it is expensive and time consuming. The present finite element model allows a comprehensive parametric study considering a wide range and combination of the parameters of interest to be investigated.

To investigate the effect of diameter to thickness ratio and uniaxial compressive strength of concrete on the behavior of confined concrete core, a combination of these two parameters is performed. Three different type of unconfined concrete compressive strength f_c (34, 44, 68 MPa) are used. For each uniaxial compressive strength of concrete a total of six different diameter to thickness ratios (*D/t*) (25, 34, 45, 60, 85, and 100) are considered.

The effect of important parameters such as the thickness of steel tube, concrete strength, length of shear bolt, diameter of shear bolts, and bolt material strength on the shear capacity and on the behavior of concrete-filled steel tube with shear connectors is investigated. Steel tube with 1.5, 3, 5, 7.1, and 10 mm thickness, concrete compressive strength f_c (34, 44, and 68 MPa), shear bolt with 8, 12, 16, and 20 mm diameter, shear bolt with 25, 45, 55, 65, and 75 mm length, and bolt type 4.6, 5.6, and 8.8 are considered. The effects of arrangement of bolts on load transfer are also investigated (Fig. 12). Nonlinear regression is used to derive nonlinear curve fitting that represents the general trend of the data, which is obtained from parametric study. This curve can be used to predict further values.

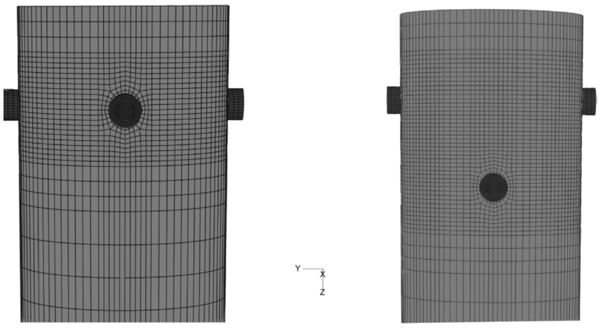

(a) (b)

Fig. 12 Bolts arrangement (a) pattern 1, (b) pattern 2

5. Results and evaluation

The axial stress and shear stress distribution on concrete core under S type of loading at the maximum bond stress are presented in Fig. 22. It can be seen that the distribution of axial stress is nearly uniform on the concrete core cross-section, and the distribution of the shear stress is uniform along the column length. The bond-slip stiffness is increased gradually toward the bottom of column. On other words, the relative slip is larger at the top of column. Therefore, the top of column is an adequate position to install the shear connectors.

Finite element analyses show that the concrete stress below the shear connectors reaches very high stress values, because of the confinement that is provided by steel tube (Fig. 23). The tests results and numerical results show that the bond stress and shear connectors work well in transferring forces between the steel tube and concrete core. Before the steel tube reaches the yield strength, the load is transferred by direct bearing pressure to the concrete. However, after reaching the yield strength, the bolts start to rotate and the bearing stresses begin to decline gradually. With the rotation of the shear connectors high frictional shear stresses are created to the effect that the load transfer is enhanced by pinching and contraction effects. The axial stresses in bolt and the stress distribution in concrete core at the maximum transferred load before yielding the steel tube are shown in Fig. 23. Fig. 24 shows the failure of concrete and steel tube deformation at the bolts region.

The passive confining pressure provided by steel tube in the top region is extremely activated under SP type of loading. The passive confining pressure is decreased gradually toward the bottom of column. This is clearly due to load transfer from the concrete to the steel tube. It is found in tests results and in FEM analyses that the maximum longitudinal stress of steel at the ultimate load is approximately 60% of the yield strength, see von Mises yield criterion in Fig. 14. The contribution of the steel tube to the total axial resistance must be taken into the account with this type of loading. Due to the confinement of the concrete core, the enhancement in the strength of concrete is approximately 38% of unconfined concrete compressive strength f_c. The structural behavior of CFTs columns under A type of loading is considerably affected by the difference between the Poisson's rations of the steel tube and concrete core. Fig. 13 shows the lateral deformation for two materials during the loading. The steel stresses at the ultimate stage are $\sigma_{sz} = 0.89 f_y$ in longitudinal direction, and $\sigma_{s\theta} = 0.18 f_y$ circumferential direction (Fig. 14). The numerical results can not capture the

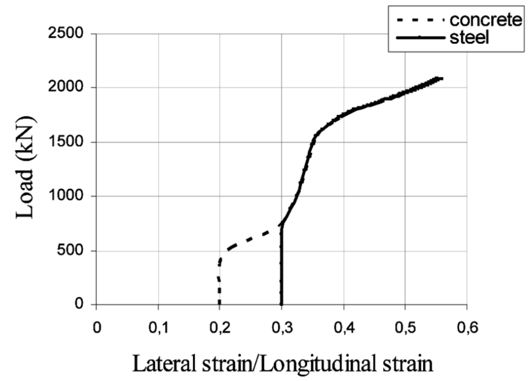

Fig. 13 Strain ratio vs. applied load in FEM-analyses

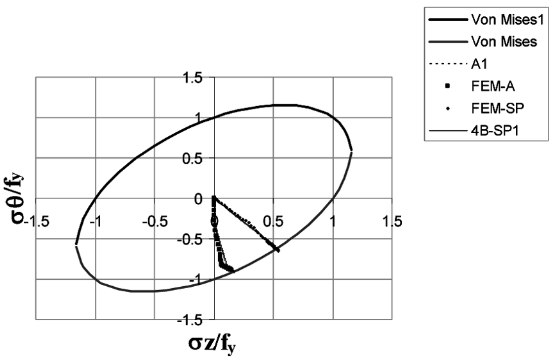

Fig. 14 Von Mises yield criterion

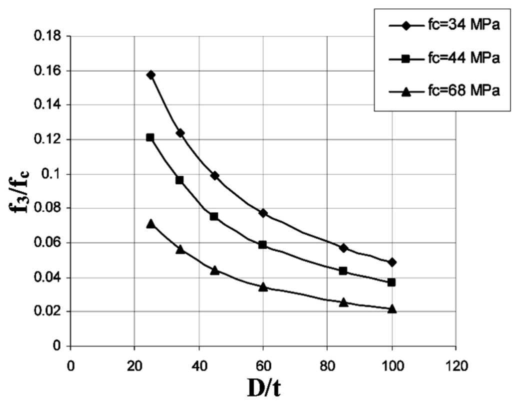

Fig. 15 The relationship between (f_3/f_c) and (D/t)

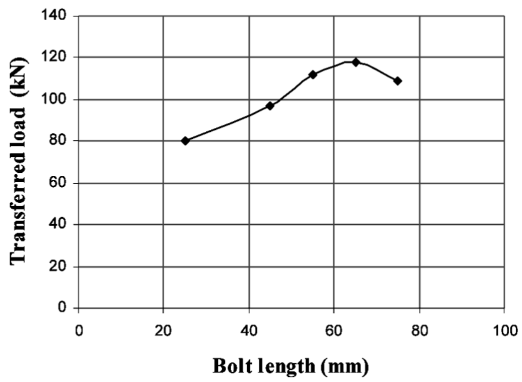

Fig. 16 Bolt length and transferred load relationship

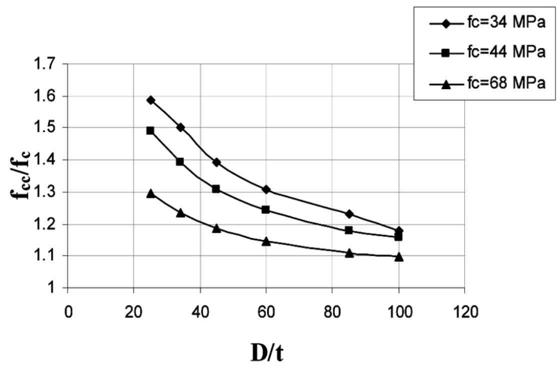

Fig. 17 The relationship between (f_{cc}/f_c) and (D/t)

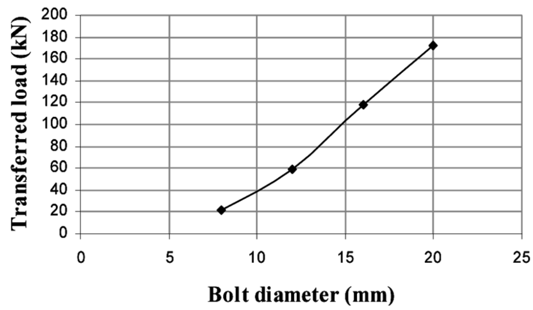

Fig. 18 Bolt diameter and transferred load relationship

behavior of columns with square cross section at a higher A type of loading level. This is due to local buckling failure of steel tube.

The results of the parameter study show that the transferred load by shear bolt increases with

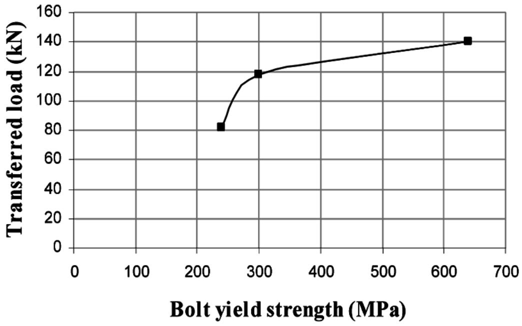

Fig. 19 Bolt yield strength and transferred load relationship

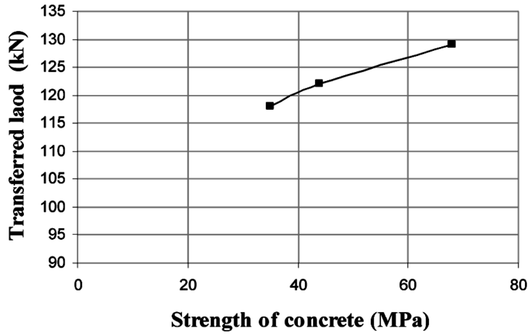

Fig. 20 Strength of concrete and transferred load relationship

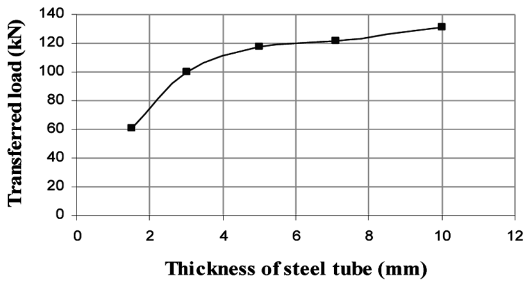

Fig. 21 Thickness of steel tube and transferred load relationship

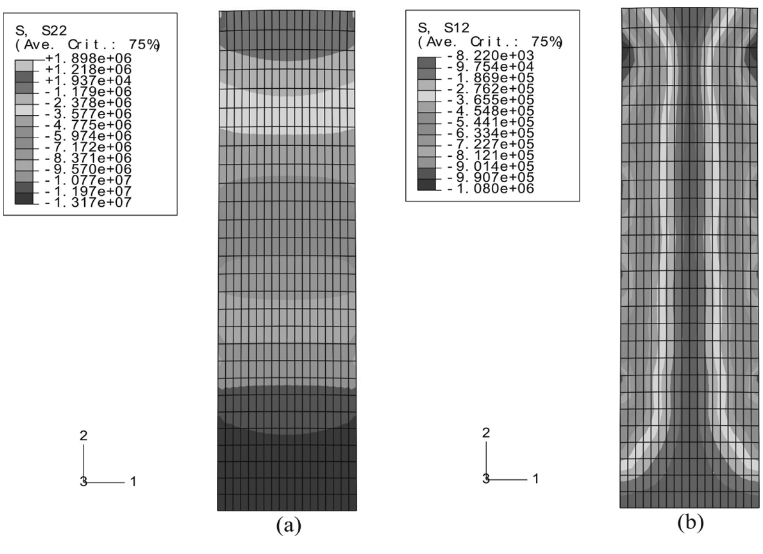

Fig. 22 Stresses in concrete at maximum bond (a) axial compression stress, (b) shear stress

increasing bolt diameter. The shear failure of bolt occurs in bolt with small diameter. However, with big cross area of bolt the steel tube reaches yield strength before occurring failure of shear bolt. The relationship between the transferred load and bolts length is shown in Fig. 16. Increasing the

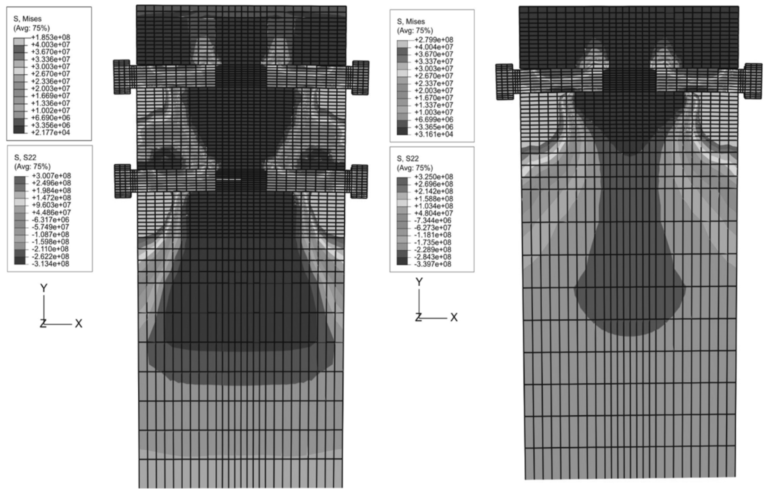

Fig. 23 Stresses in concrete and axial stresses in shear connectors

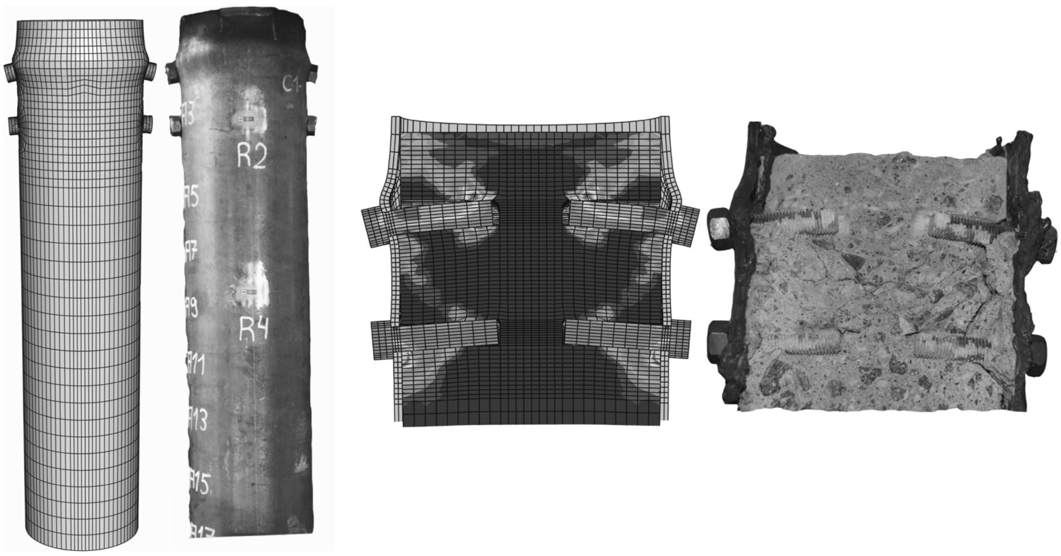

Fig. 24 Failure of specimen with shear connectors (numerical/experimental)

strength of concrete does not enhance the capacity of shear bolts to transfer the load to the concrete core with the same cross section because of the yielding of steel tube. It can be seen that the maximum load transfer is achieved with bolt length is between 50 mm and 70 mm in this type of cross section and material properties. The failure mode changes from yield of steel tube to shear failure of bolt with increasing the thickness of steel tube. It was found that, there is insignificant enhancement in the load transfer with changing the positions of the four bolts.

Fig. 17 presents the relationship between the confinement ratio (f_{cc}/f_c) and diameter to thickness ratio (D/t) for a circular CFT column. Fig. 15 presents the relationship between the lateral confinement pressure ratio (f_3/f_c) and the diameter to thickness (D/t). A more detailed account of the experimental and numerical work reported here is given by Falah (2008).

6. Conclusions

In this study, two- and three-dimensional finite element models have been developed to investigate the force transfer by natural bond or by mechanical shear connectors and the interaction between the steel tube and the concrete core of concrete-filled steel tubes under three types of loading. Both material and geometric nonlinearities are considered in the analyses. The numerical results indicate good agreement with the experimental data. The plastic damage model can be used to predict the nonlinear response of confined concrete (passive confinement effect) in CFTs columns subjected to axial compressive loading. The bond between steel tube and concrete core is simulated well using a nonlinear spring element. By means of parameter studies, it was found that the behavior and capacity of shear bolts are mainly influenced by bolt geometry, bolt material property, thickness of steel tube, and concrete core properties. For practical purposes, a minimum number of four bolts is suggested, with two bolts being placed on each side of the CFT.

Acknowledgements

The authors would like to acknowledge the contribution made by Dr. J. Priebe, Eng. A. Seils, Mr. T. Jessen, and Mr. U. Stender to the experimental work reported here.

References

Begum, M., Driver, G.R. and Elwi, E.A. (2007), “Finite-element modeling of partially encased composite columns using the dynamic explicit method”, *J. Struct. Eng-ASCE*, **133**(3), 326-334.
Bussler, T. (2007), “Numerische Untersuchungen zum Tragverhalten von Schubbolzen in Verbundstützen (Numerical investigations on the structural behavior of shear studs in composite columns)”, Diplomarbeit, Hamburg University of Technology, Germany.
Chen, W.F. (1982), *Plasticity in Reinforced Concrete*, McGraw-Hill, New York.
Ellobody, E. (2007), “Nonlinear behavior of concrete-filled stainless steel stiffened slender tube columns”, *Thin Wall. Struct.*, **45**(3), 259-273.
Falah, N. (2008), “The interaction of steel tube and concrete core in concrete-filled steel tube columns”, Doctoral Thesis in Preparation.
HKS (2007), *ABAQUS/Standard User's Manual*, Version 6.7, Hibbit, Karlsson & Sorensen, Inc., Pawtucket, USA.
Hu, H.T., Huang, C.S. and Wu, M.H. (2003), “Nonlinear analysis of axially loaded concrete-filled tube columns with confinement effect”, *J. Struct. Eng-ASCE*, **129**(10), 1322-1329.
Johansson, M. (2003), “Composite action in connection regions of concrete-filled steel tube columns”, *Steel Compos. Struct.*, **3**(1), 47-64.
Johansson, M., Claeson, C., Akesson, M. and Gylltoft, K. (2000), “Stuctural behavior of circular composite columns under various means of load application”, *Proceeding of 6th ASCCS Conference*, Los Angeles, USA.
Lam, D. and El-Lobody, E. (2005), “Behavior of head stud shear connectors in composite beam”, *J. Struct. Eng-ASCE*, **131**(1), 96-107.
Lee, J. and Fenves, G.L. (1998), “Plastic-damage model for cyclic loading of concrete structures”, *J. Eng. Mech.*, **124**(8), 892-900.
Lubliner, J., Oliver, J., Oller, S. and Oñate, E. (1989), “A plastic-damaged model for concrete”, *Int. J. Solids Struct.*, **25**(3), 299-329.
Morishita, Y., Tomii, M. and Yoshimura, K. (1979), “Experimental studies on bond strength in concrete-filled

circular steel tubular columns subjected to axial loads", *Trans. Japan Concrete Inst. Tokyo*, **1**, 351-358.

Roeder, C.W., Chmielowski, R. and Brown, C.B. (1999), "Shear connector requirements for embedded steel sections", *J. Struct. Eng-ASCE*, **125**(2), 142-152.

Roeder, C.W., Cameron, B. and Brown, C.B. (1999), "Composite action in concrete-filled tubes", *J. Struct. Eng-ASCE*, **125**(5), 477-484.

Shakir-Khalil, H. (1991), "Bond strength in hollow concrete-filled steel hollow sections", *Proceedings of the International Conference on Steel and Aluminum Structures. Composite Steel Structures*, Singapore.

Shakir-Khalil, H. (1993a), "Push-out strength of concrete-filled steel hollow sections", *Struct. Eng.,* **71**(13), 230-233, 243.

Shakir-Khalil, H. (1993b), "Resistance of concrete-filled steel hollow tubes to pushout forces", *Struct. Eng.*, **71**(13), 234-243.

Schneider, S.P. (1998), "Axially loaded concrete-filled steel tubes", *J. Struct. Eng-ASCE,* **124**(10), 1125-1138.

Shams, M. and Saadeghvaziri, M.A. (2000), "Non-linear behavior of concrete-filled steel tubular columns under axial and lateral loadings", *Proceeding of 6th ASCCS Conference,* Los Angeles, USA.

Starossek, U., Falah, N. and Löhning, T. (2008), "Numerical analyses of the force transfer in concrete-filled steel tube columns", *Proceedings of 4th International Conference on Advances in Structural Engineering and Mechanics*, Jeju, Korea, May.

Starossek, U. and Falah, N. (2008), "Force transfer in concrete-filled steel tube columns", *Proceedings of 5th European Conference on Steel and Composite Structures*, Graz, Austria, September.

Starossek, U. and Falah, N. (2008), "The interaction of steel tube and concrete core in concrete-filled steel tube columns", *Proceedings of 12th International Symposium on Tubular Structures*, Shanghai, China, October.

Virdi, K.S. and Dowling, P.J. (1980), "Bond strength in concrete-filled steel tubes", *IABSE*, **33**(80), 125-139.